Theory of Mitotic Spindle Oscillations

Stephan W. Grill,[1,*] Karsten Kruse,[2] and Frank Jülicher[2]

[1]*Max-Planck Institute for Molecular Cell Biology and Genetics, Pfotenhauerstrasse 108, 01307 Dresden, Germany*
[2]*Max-Planck-Institute for the Physics of Complex Systems, Nöthnitzerstrasse 38, 01187 Dresden, Germany*

(Received 5 November 2004; published 18 March 2005)

During unequal cell division the mitotic spindle is positioned away from the center of the cell before cell cleavage. In many biological systems this repositioning is accompanied by oscillatory movements of the spindle. We present a theoretical description for mitotic spindle oscillations. We show that the cooperative attachment and detachment of cortical force generators to astral microtubules leads to spontaneous oscillations beyond a critical number of force generators. This mechanism can quantitatively describe the spindle oscillations observed during unequal division of the one cell stage *Caenorhabditis elegans* embryo.

DOI: 10.1103/PhysRevLett.94.108104 PACS numbers: 87.17.–d, 05.45.–a, 87.16.Ka

The cytoskeleton of cells displays a wide range of dynamic processes. Examples are cell locomotion, axonemal motility, and the separation of chromosomes during cell division [1]. In the latter case, microtubules, which are filaments of the cytoskeleton, form a spindle consisting of two asters of microtubules radiating outwards from two mechanically connected poles; see Fig. 1(a). The spindle is essential to organize chromosome segregation during mitosis but also to define the constriction plane at which the original cell is divided. Here, we focus on oscillatory movements of the spindle poles which can occur during asymmetric cell divisions resulting in two daughter cells of unequal sizes. Such unequal cell divisions are essential for the generation of cell type diversity during the development of an organism [2]. The dividing cell achieves unequal sizes of the daughter cells by moving the mitotic spindle from an initial position at the geometric center of the cell towards a cell pole [3]. In many organisms, oscillations are observed during this process of spindle repositioning [4–6].

An example of unequal cell division is provided by the very first cell division in the fertilized egg of the nematode worm *C. elegans.* This division creates a larger anterior and a smaller posterior daughter cell along the anterior-posterior (AP) axis of the developing embryo [7]. Spindle displacement towards the posterior cell cortex is accompanied by pronounced oscillations of the spindle in a direction perpendicular to the AP axis [4]. It has been suggested that spindle oscillations are a direct consequence of the active processes underlying spindle repositioning [6].

The dynamics of the spindle is governed by several factors. The polymerization and depolymerization of microtubules are involved in the centering of the spindle within the cell [8]. In addition, the bending elasticity of astral microtubules provides for an elastic restoring force on the spindle if it is displaced from the center [1]. Finally, there is evidence for the existence of force generating elements on the cell cortex which can attach to astral microtubules and thus exert forces on the spindle poles [9]. The cortical force generators are likely to include molecular motors such as dyneins [5,10]. In recent experiments, spindle poles were fragmented with a UV laser, and the subsequent rates of fragment movement towards the cell cortex were determined. A statistical analysis of the mean and the variance of fragment velocities suggests that a larger number of force generators is acting on microtubules of the posterior spindle pole as compared to the anterior pole. It has been suggested that this imbalance of the number of force generators causes the spindle to displace towards the posterior cortex [9].

In this Letter, we show that the interplay of force generators stochastically binding and detaching from astral microtubules together with microtubule elasticity leads to spindle pole oscillations if the number of force generators is increased beyond a critical value. We present an analysis of the relevant forces and a physical description of the dynamics of force generators and compare our calculations to experimental observations of spindle pole oscillations. We find that a simple model can quantitatively account for the observations. Our analysis reveals essential features of

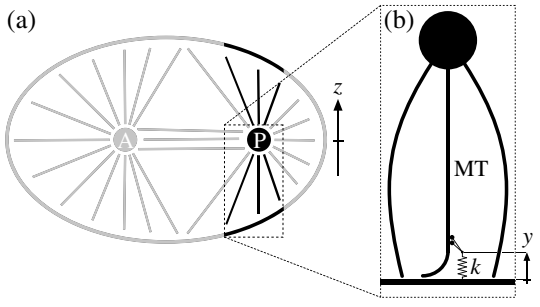

FIG. 1. (a) Schematic representation of the mitotic spindle in a single-cell stage *C. elegans* embryo. Microtubules (MT) radiate out from the anterior (A) and posterior (P) spindle poles. Cortical forces induce spindle pole displacements along the z axis. (b) Interactions of the spindle pole with the lower cortex. Force generators are attached to the cortex via elastic linkers of stiffness k. The linker extension is denoted y. The bending rigidity of unattached microtubules provides a restoring force.

the physical mechanisms underlying cortical force generation and spindle positioning.

Since oscillations are predominantly normal to the AP axis, we use a one-dimensional description and study the dynamics along the z axis; see Fig. 1. We denote by G the projection on the z axis of the total force generated by interactions between astral microtubules of one spindle pole and cortical force generators. The equation of motion of the spindle pole can be written as

$$\xi \dot{z} = -Kz + G, \tag{1}$$

where the dot denotes a time derivative, ξ is an effective friction coefficient for spindle motion inside the cell, and the stiffness K results from the bending elasticity of astral microtubules. The force G is produced by force generators located in both the upper and the lower cortex (see Fig. 1), which are assumed to contain the same number N of identical force generators. We denote by F the force generated in the lower cortex [see Fig. 1(b)]. Since force generators can attach anywhere along a microtubule, this force is independent of the absolute spindle position z. In general, F depends on the history of spindle displacements and thus can be expressed as a function of the velocity $\dot{z}$ and higher time derivatives of z, i.e., $F(\dot{z}, \ddot{z}, \ldots)$. The force generators of the upper cortex act in the opposite direction and are subject to displacements $-z(t)$. Therefore the total force exerted by force generators on both sides reads

$$G(\dot{z}, \ddot{z}, \ldots) = F(\dot{z}, \ddot{z}, \ldots) - F(-\dot{z}, -\ddot{z}, \ldots), \tag{2}$$

which is antisymmetric with respect to $\dot{z}(t) \rightarrow -\dot{z}(t)$.

We calculate the cortical force F generated in the lower cortex by assuming that each force generator is linked to the cell cortex via an elastic linker of stiffness k. Denoting the linker extension by y (see Fig. 1(b)), the cortical force is given by $F = -k\sum_{i=1}^{N_b} y_i$, where N_b is the number of force generators attached to microtubules and y_i their individual linker lengths. Force generators are characterized by a force-velocity relationship that describes the velocity v of motion of a force generator along a microtubule as a function of a force f acting on the force generator in a direction opposing this motion [1]. We choose for simplicity a linear relation $v = v_0 - f v_0/f_0$. Here, f_0 is the stall force at which motion stops, and v_0 denotes the spontaneous velocity in the absence of forces. In the present case, the load force $f = ky$ is the force exerted by the elastic linker with extension y. For a force generator bound to a microtubule, the linker length thus changes with a velocity

$$\dot{y} = v_0 - \mu y + \dot{z}, \tag{3}$$

where $\mu = k v_0/f_0$. In addition, unbound force generators stochastically attach to microtubules at a rate ω_{on}, and bound force generators detach at a rate ω_{off}. These rates, in general, depend on the load force and thus on the linker length y.

We introduce the probability density $P_b(y)$ for a given force generator with linker length y to be bound to a microtubule. For a sufficiently large number of force generators, the force exerted on the spindle pole can be approximated as the average

$$F = -Nk \int_{-\infty}^{\infty} y P_b(y) dy. \tag{4}$$

We furthermore introduce the probability density $P_u(y)$ of unbound force generators. These probability distributions obey

$$\partial_t P_b + \partial_y J_b = \omega_{\mathrm{on}} P_u - \omega_{\mathrm{off}} P_b, \tag{5}$$

$$\partial_t P_u + \partial_y J_u = -\omega_{\mathrm{on}} P_u + \omega_{\mathrm{off}} P_b. \tag{6}$$

The probability currents of bound and unbound force generators read

$$J_b = \dot{y} P_b - D_b \partial_y P_b, \tag{7}$$

$$J_u = -\nu y P_u - D_u \partial_y P_u, \tag{8}$$

where D_u is a diffusion coefficient and ν the relaxation rate of unbound force generators. Velocity fluctuations of attached force generators are characterized by the coefficient D_b. The distributions P_b and P_u are normalized: $\int_{-\infty}^{\infty}(P_b + P_u)dy = 1$.

The relaxation rate of detached force generators is fast compared to the rate ω_{on} of rebinding. We assume for simplicity that force generators relax instantaneously after detachment to an equilibrium distribution

$$P_u = Q_u(t) A \exp\left\{-\frac{k y^2}{2 k_B T}\right\}, \tag{9}$$

where $A = [k/(2\pi k_B T)]^{1/2}$ and Q_u is the fraction of unbound force generators. Integrating Eq. (6) with respect to y leads to

$$\frac{d}{dt} Q_u = -\bar{\omega}_{\mathrm{on}} Q_u + \int_{-\infty}^{\infty} \omega_{\mathrm{off}} P_b(y) dy, \tag{10}$$

where $\bar{\omega}_{\mathrm{on}} = A \int_{-\infty}^{\infty} \omega_{\mathrm{on}}(y) \exp\{-k y^2/(2 k_B T)\} dy$ is the average attachment rate.

In order to complete the equations, we specify the stress dependence of the detachment rate by

$$\omega_{\mathrm{off}} = \omega_0 \exp\left\{\frac{k a |y|}{k_B T}\right\}. \tag{11}$$

Here, ω_0 is the detachment rate in the absence of forces and a denotes a molecular length scale. This expression is consistent with experiments on single kinesin molecules [11–13] and is a simple approximation for a more detailed calculation [14].

Many of the values of parameters in the dynamic equations can be estimated using known properties of microtubules and cytoskeletal motor proteins. We choose $v_0 \simeq 1.8\ \mu$m/s and $f_0 \simeq 3$ pN, consistent with mechanical properties of dynein motor proteins [1,15] and observed velocities in *C. elegans* embryos [9,15]. Observed oscillations are almost sinusoidal [see Fig. 2(c)]. Therefore velocity variations are expected to be rather small and force

generators thus are unlikely to reach their maximal velocity. Hence we assume force generators to operate near stall, implying a rather rapid relaxation rate μ. We choose $\mu \simeq 50\ \mathrm{s}^{-1}$, corresponding to $k \simeq 8 \times 10^{-5}$ N/m. The time a force generator spends attached to a filament in the absence of forces determines the rate ω_0. Here we choose $\omega_0 \simeq 0.05\ \mathrm{s}^{-1}$ in order to match the amplitude and the frequency of the observed oscillations. The force dependence of detachments is determined by the molecular length scale $a \simeq 3$ nm. A rough estimate for the drag coefficient of spindle pole motion can be obtained using Stokes friction for an object of several micrometers in size. Using an effective viscosity of 10 times the viscosity of water for the intracellular medium, we choose $\xi \simeq 10^{-6}$ N s/m. Finally, the elastic modulus K for spindle pole displacements is unknown. We use a value of $K \simeq 4 \times 10^{-6}$ N/m, which is consistent with microtubule elasticity and generates the observed amplitude and frequency of oscillations.

We numerically solve Eqs. (1), (4), (5), and (10), taking into account two separate collections of force generators in the upper and the lower cortex; see Eq. (2). An example of spontaneous oscillations for $N = 30$ in this system is displayed in Fig. 2(a). This number of force generators is consistent with previous estimates [9]. Oscillations have the same amplitude and frequency as observed in oscillating mitotic spindles in *C. elegans* [Fig. 2(c)]. In general, we find that oscillations occur for a sufficiently large number of force generators and within a range of attachment rates $\bar{\omega}_{\mathrm{on}}$. Figure 3 shows the corresponding state diagram indicating a region of spontaneous oscillations separated from the nonoscillating regime by a line of oscillatory instabilities. Here we have varied the parameters N and $\bar{\omega}_{\mathrm{on}}$ since they control the number of active force generators. This number has been suggested to be the relevant quantity controlled by the cell to displace the spindle [9].

In Eq. (4), fluctuations in the number of active force generators are neglected. For small N these fluctuations become important and lead to noisy oscillations. Experimentally observed oscillations are indeed noisy; see Fig. 2(c). In order to verify that oscillations still occur in the presence of force fluctuations, we performed stochastic computer simulations where $N = 30$ force generators individually bind to and detach from microtubules in the upper and the lower cortex. An example of the resulting noisy oscillations is shown in Fig. 2(b).

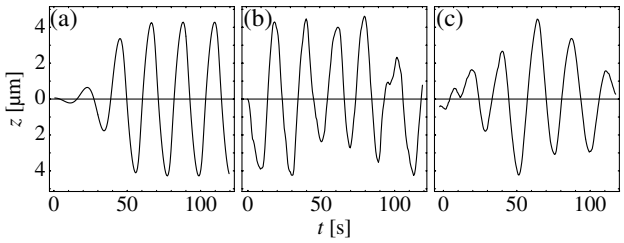

FIG. 2. Spindle pole position z as a function of time t. (a) Numerical solution to Eqs. (4)–(7) with $D_b = 5 \times 10^{-15}\ \mathrm{m}^2/\mathrm{s}$. (b) Stochastic simulation of individual force generators. (c) Experimentally measured positions of the posterior spindle pole. Parameter values used in (a) and (b) are $v_0 = 1.8\ \mu$m/s, $f_0 = 3$ pN, $k = 8.3 \times 10^{-5}$ N/m, $\omega_0 = 0.05\ \mathrm{s}^{-1}$, $\xi = 10^{-6}$ N s/m, $K = 4 \times 10^{-6}$ N/m, $\bar{\omega}_{\mathrm{on}} = 0.25\ \mathrm{s}^{-1}$, and $N = 30$.

In order to obtain a physical understanding of the oscillations, we discuss a simple approximation to the dynamic equations which captures the essential features of motor action. We replace the distribution $P_b(y)$ of the linker lengths of bound force generators by a typical linker length $\bar{y}$. The total force exerted by the force generators on the lower cortex can then be written as $F \simeq -NQ_b k\bar{y}$, where $Q_b = \int P_b dy = 1 - Q_u$ is the fraction of bound force generators.

The value of $\bar{y}$ is estimated as the typical distance a force generator advances before it detaches. This distance is given by $\bar{y} \simeq \dot{y}/\omega_{\mathrm{off}}$. The spindle pole velocity then reads [Eq. (3)]

$$\dot{z} = [\omega_{\mathrm{off}}(\bar{y}) + \mu]\bar{y} - v_0. \tag{12}$$

The linker length $\bar{y}$ as a function of $\dot{z}$ results from inverting this expression. The simplified dynamic equations are completed by

$$\frac{d}{dt}Q_b = \bar{\omega}_{\mathrm{on}} - [\bar{\omega}_{\mathrm{on}} + \omega_{\mathrm{off}}(\bar{y})]Q_b, \tag{13}$$

which follows from Eq. (10) and includes the approximation $\omega_{\mathrm{off}}(\bar{y}) \simeq \int \omega_{\mathrm{off}} P_b dy$.

These equations have a steady state solution with resting spindle pole at $z = 0$ with constant $Q_b = Q_b^{(0)}$ and $\bar{y} = \bar{y}_0$. The possibility of spontaneous oscillations is revealed by a linear stability analysis. Inserting the ansatz $Q_b \simeq Q_b^{(0)} + Q_b^{(1)} e^{-st}$, $\bar{y} \simeq \bar{y}_0 + \bar{y}_1 e^{-st}$, and $z \simeq z_1 e^{-st}$ in the simplified dynamic equations, we determine $s = \tau + i\omega$ which characterizes the relaxation rate τ and oscillation frequency ω. The system becomes unstable and starts to oscillate when τ changes sign and becomes negative. The total motor force is given to linear order in the spindle pole velocity $\dot{z} \simeq -sz_1 e^{-st}$ by $G \simeq -\chi(s) s z_1 e^{-st}$, where the linear response function of the cortical force generators is

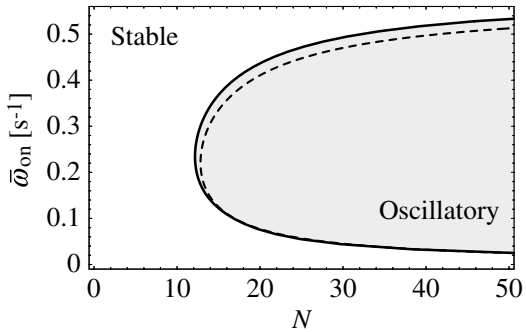

FIG. 3. State diagram of mitotic spindle dynamics. The line of instability for the full (solid line) and the simplified (broken line) equations is shown. The full equations result in oscillating solutions inside the shaded region, while the nonoscillating solution is stable outside.

$$\chi(s) = 2NkQ_b^{(0)}\left(\frac{\bar{y}_0\omega'_{\rm off}}{\bar{\omega}_{\rm on} + \omega_{\rm off}(\bar{y}_0) - s} - 1\right)\bar{y}', \qquad (14)$$

with $\bar{y}' = d\bar{y}/d\dot{z}$ at $\dot{z} = 0$ and $\omega'_{\rm off} = d\omega_{\rm off}/d\bar{y}$ at $\bar{y} = \bar{y}_0$. The relaxation rate τ and oscillation frequency ω follow from the relation $\chi(s) = \xi - K/s$. This analysis reveals the existence of a Hopf bifurcation for a critical number

$$N^* = \frac{K + \xi(\bar{\omega}_{\rm on} + \omega_{\rm off})}{2kQ_b^{(0)}\bar{y}'(\bar{y}_0\omega'_{\rm off} - \bar{\omega}_{\rm on} - \omega_{\rm off})} \qquad (15)$$

of cortical force generators with a frequency

$$\omega^* = \sqrt{\frac{K(\bar{\omega}_{\rm on} + \omega_{\rm off})}{\xi + 2NkQ_b^{(0)}\bar{y}'}} \qquad (16)$$

of oscillations at the instability. The state diagram, characterized by the dependence of N^* on the attachment rate $\bar{\omega}_{\rm on}$ is displayed in Fig. 3 by a broken line. The figure shows that the line of instability for the full dynamic equations agrees closely with the one for the simplified equations.

In conclusion, the physical mechanism for mitotic spindle oscillations in *C. elegans* proposed here relies on load-dependent detachment rates and on a restoring force. We find that oscillations occur via a supercritical Hopf bifurcation at a critical number of force generators. Spindle displacements along the AP axis are expected to result from an imbalance of the forces exerted by cortical force generators at the anterior and posterior cortex. If the number of force generators remains below the critical number N^*, our results suggest that spindle displacement would occur in the absence of oscillations. This prediction is in contrast to the assumption on which the kinetic model of Ref. [6] is based, that spindle oscillations are required for spindle displacements.

Why does the spindle oscillate during unequal cell division even though oscillations do not seem to be necessary? Spindle displacements rely on an imbalance of forces on the anterior and posterior sides. Although spindle displacement could occur for $N < N^*$, larger numbers may be advantageous for robust displacement. As the number of force generators is increased beyond N^*, oscillations become unavoidable. Indeed, the cell might even use the occurrence of spindle oscillations as an indicator for sufficient force generation.

Oscillations decay after a few periods [Fig. 2(c)], which is likely due to a general change in the state of the cell as it proceeds through mitosis. However, the stability diagram in Fig. 3 offers another possible explanation: By increasing the attachment rate instead of the number of force generators, the stationary state will be restabilized when this rate is increased beyond a critical value.

Our work shows how a collection of motors can generate oscillations via a force-dependent detachment rate. This mechanism is related to earlier discussions of motor induced oscillations [16,17] and to the saltatory motion of beads which grow an actin comet tail [18–20]. The situation discussed here applies to any "tug of war" scenario, for example, to situations where motors of opposite directionality pull an object along the same filament [21]. Our analysis shows that explicit coordination between motors acting in opposite directions is not required for switchlike or oscillatory behaviors to emerge. Load-dependent detachment rates are sufficient to generate situations where one population of motors pulls in one direction while the unproductive population of motors with opposite directionality remains detached.

We thank Joe Howard and Tony Hyman for stimulating collaborations and Joe Howard for a critical reading of the manuscript.

*Present address: Department of Physics, University of California, 175 Le Conte Hall, Berkeley, CA 94720, USA.

[1] J. Howard, *Mechanics of Motor Proteins and the Cytoskeleton* (Sinauer Associates, Sunderland, 2001).
[2] H. R. Horvitz and I. Herskowitz, Cell **68**, 237 (1992).
[3] R. Rappaport, Int. Rev. Cytol. **31**, 169 (1971).
[4] D. Albertson, Dev. Biol. **101**, 61 (1984).
[5] E. Yeh, C. Yang, E. Chin, P. Maddox, E. D. Salmon, D. J. Lew, and K. Bloom, Mol. Biol. Cell **11**, 3949 (2000).
[6] S. W. Grill, P. Gönczy, E. H. K. Stelzer, and A. A. Hyman, Nature (London) **409**, 630 (2001).
[7] K. J. Kemphues and S. Strome, in *C. elegans II*, edited by D. L. Riddle, T. Blumenthal, B. J. Meyer, and J. R. Priess (Cold Spring Harbor Laboratory Press, Cold Spring Harbor, NY, 1997), p. 335.
[8] M. Dogterom and B. Yurke, Phys. Rev. Lett. **81**, 485 (1998).
[9] S. W. Grill, J. Howard, E. Schäffer, E. H. K. Stelzer, and A. A. Hyman, Science **301**, 518 (2003).
[10] D. L. Dujardin and R. B. Vallee, Curr. Opin. Cell Biol. **14**, 44 (2002).
[11] C. M. Coppin, D. W. Pierce, L. Hsu, and R. D. Vale, Proc. Natl. Acad. Sci. U.S.A. **94**, 8539 (1997).
[12] K. Visscher, M. J. Schnitzer, and S. M. Block, Nature (London) **400**, 184 (1999).
[13] M. J. Schnitzer, K. Visscher, and S. M. Block, Nat. Cell Biol. **2**, 718 (2000).
[14] A. Parmeggiani, F. Jülicher, L. Peliti, and J. Prost, Europhys. Lett. **56**, 603 (2001).
[15] P. Gönczy, S. Pichler, M. Kirkham, and A. A. Hyman, J. Cell Biol. **147**, 135 (1999).
[16] C. Brokaw, Proc. Natl. Acad. Sci. U.S.A. **72**, 3102 (1975).
[17] F. Jülicher and J. Prost, Phys. Rev. Lett. **78**, 4510 (1997).
[18] F. Gerbal, P. Chaikin, Y. Rabin, and J. Prost, Biophys. J. **79**, 2259 (2000).
[19] J. Prost, in *Physics of Bio-molecules and Cells*, edited by H. Flyvbjerg, F. Jülicher, P. Ormos, and F. David (EDP Sciences, Les Ulis, 2001), p. 215.
[20] A. Bernheim-Groswasser, S. Wiesner, R. M. Goldsteyn, M.-F. Carlier, and C. Sykes, Nature (London) **417**, 308 (2002).
[21] S. P. Gross, M. A. Welte, S. M. Block, and E. F. Wieschaus, J. Cell Biol. **156**, 715 (2002).